J. Plasma Phys. (2021), *vol*. 87, 905870610
Published by Cambridge University Press

doi:10.1017/S0022377821001173

The fast transit-time limit of magnetic pumping with trapped electrons

J. Egedal [1],† **and E. Lichko** [2]

[1]Department of Physics, University of Wisconsin–Madison, 1150 University Avenue, Madison, WI 53706, USA

[2]Lunar and Planetary Laboratory, 1629 E University Boulevard, Tucson, AZ 85721, USA

(Received 21 May 2021; revised 2 November 2021; accepted 3 November 2021)

Recently, the energization of superthermal electrons at the Earth's bow shock was found to be consistent with a new magnetic pumping model derived in the limit where the electron transit time is much shorter than any time scale governing the evolution of the magnetic fields. The new model breaks with the common approach of integrating the kinetic equations along unperturbed orbits. Rather, the fast transit-time limit allows the electron dynamics to be characterized by adiabatic invariants (action variables) accurately capturing the nonlinear effects of electrons becoming trapped in magnetic perturbations. Without trapping, fast parallel streaming along magnetic field lines causes the electron pressure to be isotropized and homogeneous along the magnetic field lines. In contrast, trapping permits spatially varying pressure anisotropy to form along the magnetic field lines, and through a Fermi process this pressure anisotropy in turn becomes the main ingredient that renders magnetic pumping efficient for energizing superthermal electrons. We here present a detailed mathematical derivation of the model.

Key words: Plasmas

1. Introduction

Throughout the universe, energetic electrons represent the main source of electromagnetic radiation providing an important window into space and astrophysical phenomena. Given the low collisionality common to astrophysical settings, the distributions of the constituent particles are typically far from thermodynamic equilibrium, and can deviate from Maxwellians often with the formation of energetic power-law tails where $f \propto v^{-\gamma}$. Determining the physical mechanism(s) which heats electrons and produces the common power-law signature is still an unresolved problem that is at the heart of the present analysis. Following the results reported in Lichko & Egedal (2020), we here present a detailed derivation of a model for superthermal electron energization via magnetic pumping. Magnetic pumping is known as a heating mechanism that transfers energy from magnetic fluctuations to a plasma and is most effective at the largest scale of the magnetic perturbations. In the present work we show that electron trapping renders

† Email address for correspondence: egedal@wisc.edu

magnetic pumping effective for superthermal electrons, and the mechanism can then bypass the turbulent cascade and directly energize the electrons through this Fermi process that is consistent with the formation of power-law tails.

Magnetic pumping is a well-known heating mechanism and was first proposed by Hannes Alfvén as a possible way to explain observations of cosmic rays (Alfven 1950). The idea was extensively investigated as a possible heating mechanism for fusion plasmas Schluter (1957). In the analysis by Berger (1958), magnetic pumping in the regime of low collisionallity was also considered and it was found that magnetic perturbations evolving at the time scale of a particle transit time will also provide effective heating of the plasma. As such, even in the collisionless limit, magnetic pumping is a common process, related to transit-time damping (Barnes 1966). For tokamaks its implementation is hindered by the difficulty of perturbing the strong torodial field, but pumping may be feasible in other configurations operating at a higher values of the normalized plasma pressure, $\beta = 2\mu_0 nT/B^2$ (Egedal *et al.* 2018). For the low collisional condition of the solar wind ions, Lichko *et al.* (2017) developed a kinetic description to characterize the changes in the ion distribution function and found that magnetic pumping is consistent with the formation of a power-law distribution for ion energies below a critical energy related to the magnetic-field-aligned phase velocity of the magnetic perturbations, $\mathcal{E}_c = \frac{1}{2} m_i(\omega/k_{||})^2$. The model may also be applied to electrons, but, given the low electron mass, the associated critical energy, $\mathcal{E}_c = \frac{1}{2} m_e(\omega/k_{||})^2$, is generally too small compared with T_e for 'standard' magnetic pumping to become important.

To elucidate the physical mechanism of transit-time damping, Stix (1992) considers the particular case of the magnetosonic wave and describes how transit-time damping is a Landau damping process, where the energization is limited to particles moving at the magnetic-field-aligned phase velocity of the wave considered. Applying the guiding centre limit, Stix (1992) noted the mathematical similarity between the mirror force $m(\partial v_\parallel/\partial t) = -\mu \boldsymbol{b}\cdot\nabla B$ and the electrical force $m\partial v_\parallel/\partial t = e\boldsymbol{b}\cdot\boldsymbol{E}$. For a plasma with a background magnetic field B_0, it follows that $\mu(B-B_0)/e$ is equivalent to the wave electric potential in a one-dimensional plasma configuration. Transit-time damping can then be cast in a framework analogous to that applied for Landau damping of electrostatic waves. Here, using the approach of linearizing the kinetic equation through a small-amplitude expansion, $f = f_0 + f_1 + \cdots$, the standard method of integration along unperturbed particle orbits yields an approximate solution for the perturbed distribution, $m(\omega - kv_\parallel)f_1 = \mathrm{i}\mu(B-B_0)\partial f_0/\partial v_\parallel$. From this expression it becomes evident why transit-time damping is effective for ions, where typically $\partial f_0/\partial v_\parallel|_{\omega/k}$ is large yielding a large response in f_1 at the resonance velocity, $v_\parallel = \omega/k$. This resonance then becomes the driver of quasi-linear diffusion and Landau damping. Meanwhile, applying the same framework to thermal and superthermal electrons where $v_\parallel \gg \omega/k$, there are no resonances such that $f_1 \simeq (-\mathrm{i}\mu(B-B_0)/kv_\parallel)\partial f_0/\partial v_\parallel$. The large streaming velocity, $v_\parallel$, in the denominator causes f_1 to be small and effectively eliminates the possibility of electron energization by magnetic pumping.

In stark contrast to these previous results, a generalized pumping model was recently introduced by Lichko & Egedal (2020). This model also applies a small-amplitude expansion of f, but, as a main difference from previous work, the underlying kinetic equation is not integrated along unperturbed orbits. Rather, guided by *in situ* MMS spacecraft observations recorded at the Earth's bow shock, the model includes the effects of electron trapping in compressional magnetic perturbations. As a heuristic argument as to why trapping is important, for the case of unperturbed orbits, the effective interaction time of the electrons with the perturbation is of the order of $1/(kv_\parallel)$. Meanwhile for trapped electrons the typical interaction time becomes much longer (of the order of $1/\omega$)

https://doi.org/10.1017/S0022377821001173 Published online by Cambridge University Press

such that the energizing of term $\mu\partial B/\partial t$ yields significant changes in the electron kinetic energies during the course of a single magnetic perturbation. Pitch angle mixing can randomize the energization, which through μ is proportional to the particle initial energy, and magnetic pumping with trapped electrons then becomes a second-order Fermi heating process, fully consistent with the formation of power-law electron distributions. Given the ubiquity of magnetic perturbations in both heliospheric and astrophysical plasmas, magnetic pumping with trapped electrons has the potential to become transformative to our understanding of how the most energetic particles in the universe may be generated. It should be emphasized that the present analysis applies a prescribed and highly idealized magnetic perturbation. As such, further work is required to generalize the results to more general configurations including parallel velocity mixing (Egedal, Schroeder & Lichko 2021) and to characterized the feedback/damping of the energization process on the magnetic perturbations.

Following the blueprint of the framework for quasi-linear diffusion, in this paper we provide a rigorous mathematical derivation of the magnetic pumping model first introduced by Lichko & Egedal (2020) applicable to the fast transit-time limit of superthermal electrons including the effects of electron trapping. The paper is organized as follows. In § 2 we introduce the action integral $J = \oint v_\parallel \, \mathrm{d}l$ which is an adiabatic invariant and show how J together with μ provide a solution so the kinetic response of electrons in a standing magnetic perturbation. The important role of pitch angle diffusion to the effectiveness of magnetic pumping is discussed in § 3 and the form of the applied drift-kinetic model is described in § 4. Section 5 introduces a Krook scattering operator, which is applied in § 6, where, as the main result of the analysis, the new model for magnetic pumping is formally derived. The paper is concluded in § 7.

2. Pressure anisotropy in the limits of fast transit time and no pitch angle scattering

In the present analysis we consider electrons sufficiently energetic that compared with $e\boldsymbol{v} \times \boldsymbol{B}$ the force of the electric field becomes unimportant to their single-pass guiding centre orbit motion. This restricts the study to superthermal electrons for which $\mathcal{E} \gg e\Phi$, where $\Phi \simeq T_e/e$ is the electrostatic potential. Given the low electron mass, the electron thermal motion is often sufficiently fast that each electron transit occurs on a time scale that is much faster than the time scale characterizing the evolution of the magnetic field. Considering this fast transit-time limit, the first and second adiabatic invariants, $\mu = m{v_\perp}^2/(2B)$ and $J = \oint v_\parallel \, \mathrm{d}l$, respectively, are conserved quantities. We also assume a two-dimensional periodic system, without gradients in the y direction, i.e. $\partial/\partial y = 0$. In the drift-kinetic limit (assuming a low electron mass) the electrons then strictly follow the contours of constant magnetic flux, $\Psi = A_y(x, z)$. Here $A_y(x, z)$ is the y component of the magnetic vector potential, and assuming $B_y = 0$, the magnetic field is given by $\boldsymbol{B} = \nabla A_y \times \boldsymbol{e}_y$, where $\boldsymbol{e}_y$ is the unit vector in the y direction.

The framework is readily generalized to other geometries as long as only a single local maximum is present in B within the periodic domain considered. As shown by Egedal *et al.* (2021), multiple local maxima in B are associated with separate locally trapped populations and in a dynamically changing configuration orbit transitions can lead to energization through $v_\parallel$ mixing. This effect of energization by mixing of separate trapped populations is not addressed here.

To illustrate how anisotropic features in $f(\boldsymbol{x}, \boldsymbol{v})$ are generated during magnetic perturbations, we consider the simple compressional perturbation shown in figure 1, where x represents the position along the flux tube. We introduce $\tilde{B}_m(t)$ as the maximum field strength observed along the flux tube, normalized by the background field B_0. Thus, for

https://doi.org/10.1017/S0022377821001173 Published online by Cambridge University Press

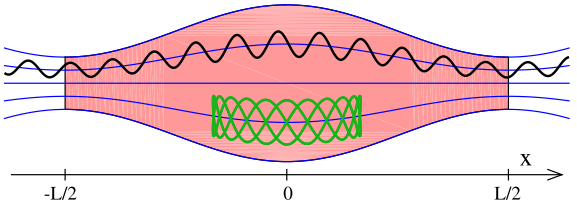

FIGURE 1. A trapped (green) and a passing (black) electron orbit within a compressional magnetic perturbation.

sinusoidal and periodic perturbations of amplitude ΔB and angular frequency ω, we have

$$\tilde{B}_m(t) = 1 + (\Delta B/B_0)|\sin(\omega t)|. \tag{2.1}$$

The spatial and temporal evolution of the normalized magnetic field is then described by

$$\tilde{B}(x, t) = 1 - (\tilde{B}_m(t) - 1)\cos(k_\parallel x). \tag{2.2}$$

As indicated in figure 1, we consider the section of the flux tube with $-L/2 \le x \le L/2$, where $L = 2\pi/k_\parallel$, and with values of $\tilde{B}$ characterized by the range $2 - \tilde{B}_m \le \tilde{B} \le \tilde{B}_m$.

The limit of negligible pitch angle scattering is conveniently explored using the adiabatic invariants μ and J. For the present geometry the orbits can be categorized as either trapped or passing as illustrated in figure 1, and we define the action integral as

$$J = 4\int_0^{L_b} v_\parallel \, \mathrm{d}x', \tag{2.3}$$

where for trapped particles L_b is the location of the particle turning point, while $L_b = L/2$ for passing electrons. For trapped orbits the factor of 4 in front of the integral corresponds to the four sections of the full orbits with alternating signs of $xv_\parallel$. For the case of passing electrons the factor of 4 results when counting contributions from orbits with both signs of $v_\parallel$ (but otherwise identical values of μ and $\mathcal{E}$), making the definition of J in (2.3) continuous across the trapped–passing boundary.

We first consider the limit of negligible pitch angle scattering, and assume that the initial distribution function $f = f_0(v^2)$ is isotropic along the uniform flux tube $\tilde{B} = 1$ observed at $t = 0$. It is now useful to introduce the normalized action integral and the so-called pitch angle variable, respectively defined by

$$j = \frac{1}{2Lv}J, \quad \Lambda = \frac{\mu B_0}{\mathcal{E}}. \tag{2.4a,b}$$

For $t = 0$, where the flux tube is uniform with $B = B_0$, we find that $j = v_\parallel/v$ and $\Lambda = {v_\perp}^2/v^2$, such that for this particular time $v^2 = v^2(j^2 + \Lambda)$. The distribution function during the evolution of the magnetic perturbation can then simply be expressed as

$$f(x, v_\parallel, v_\perp, t) = f_0(v^2(j^2 + \Lambda)). \tag{2.5}$$

This result follows directly from Jean's theorem (Jeans 1915) stating that $f = g(\mu, J)$ is a solution to the kinetic equation for an arbitrary function g, where we note that $v^2(j^2 + \Lambda) = (J/(2L))^2 + 2\mu B_0/m_e$ is a simple function of these invariants, and that (2.5) reproduces the initial condition of $f = f_0(v^2)$ for $t = 0$.

https://doi.org/10.1017/S0022377821001173 Published online by Cambridge University Press

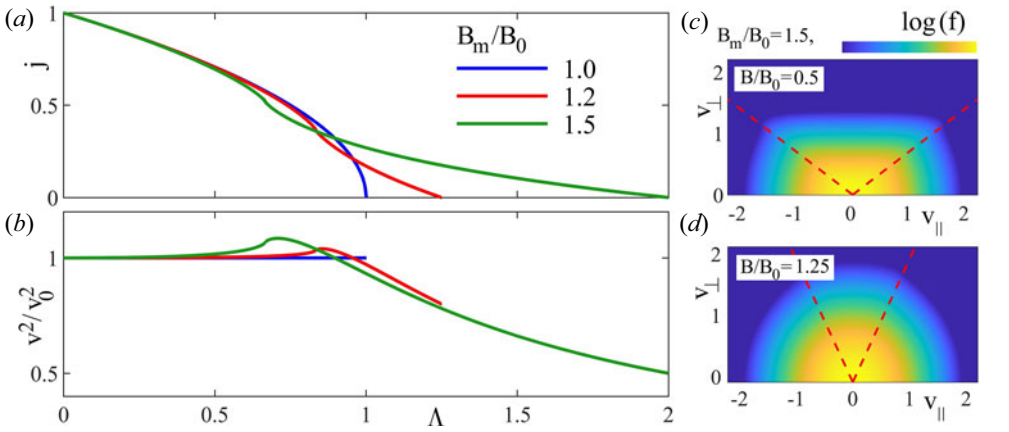

FIGURE 2. (*a*) The function $j(\Lambda)$ in (2.6) plotted as a function of Λ and evaluated for three separate values of $\tilde{B}_m$. (*b*) The relative particle energization $v^2/v_0^2 = 1/(j^2 + \Lambda)$. (*c*,*d*) Examples of local electron distributions predicted by (2.5) both computed for $B_m/B_0 = 1.5$, and a Maxwellian f_0 with thermal speed $v_t = 1$. In (*c*) the local position is at the point of minimum field strength, $B/B_0 = 0.5$, whereas $B/B_0 = 1.25$ for the distribution in (*d*).

For a given point in the configuration space $(x, v_\parallel, v_\perp, t)$ the values of Λ and j are readily evaluated. For this, we notice that

$$j(\Lambda, t) = \frac{2}{L}\int_0^{L_b} \frac{v_\parallel}{v}\mathrm{d}x' = \frac{2}{L}\int_0^{L_b} \sqrt{1 - \Lambda\tilde{B}(x', t)}\,\mathrm{d}x'. \tag{2.6}$$

Here, for any time t, the bounce points of trapped electrons are obtained from the condition $\Lambda\tilde{B}(L_b, t) = 1$, such that j is independent of v and a function of only (Λ, t). With Λ determined by the local values of $v_\parallel$, $v_\perp$ and $B(x, t)$, numerical integration of (2.6) then provides all the information required for evaluation of $f(x, v_\parallel, v_\perp, t)$ in (2.5).

The function $j(\Lambda, t)$ in (2.6) is also fundamental to the pumping model to be developed in the following sections, and figure 2(*a*) shows $j(\Lambda)$ computed for $\tilde{B}_m = 1$, 1.2 and 1.5. A value of $\Lambda = 0$ is characteristic of passing orbits with $|v_\parallel/v| = 1$, and given the normalization in (2.6) we have $j = 1$. Because $B_{\min}/B_0 = 2 - \tilde{B}_m(t)$ is a function of time, the maximum value of Λ, which we denote $\Lambda_m = B_0/B_{\min}$, also changes in time. For example, for $\tilde{B}_m = 1$, we find $j = \sqrt{1 - \Lambda}$, and we have $\Lambda_m = 1$. Meanwhile, for the green curve in figure 2(*a*) for $\tilde{B}_m = 1.5$, we observe $\Lambda_m = 2$. For any geometry, the most deeply trapped electrons are those with $\Lambda = \Lambda_m$, corresponding to $v_\parallel/v = 0$, such that $j(\Lambda_m, t) = 0$ for all values of t.

The increase in particle energy during the evolution of the magnetic perturbation can also be deduced from the expression in (2.5). By Liouville mapping, the argument of f_0 must be v_0^2, such that $v_0^2 = v^2(j^2 + \Lambda)$. It follows that the relative energization is $\mathcal{E}/\mathcal{E}_0 = v^2/v_0^2 = 1/(j^2 + \Lambda)$, and is in figure 2(*b*) plotted as a function of Λ for the same three values of $\tilde{B}_m$ considered in figure 2(*a*). For $\tilde{B}_m = 1$ there is naturally no heating and $v^2/v_0^2 = 1$. For $\tilde{B}_m > 1$, depending on the value of Λ both heating and cooling are observed, and as discussed next, energization is observed for electrons near the trapped–passing boundary, whereas the cooling is most significant for deeply trapped electrons.

https://doi.org/10.1017/S0022377821001173 Published online by Cambridge University Press

Physically, the form of f in (2.5) is the result of electron heating proportional to $\mu\,\langle\partial B/\partial t\rangle_{\rm orbit}$, where μ is the electron magnetic moment. We can use this insight to account for the anisotropic features observed in the theoretical distributions displayed in figure 2(*c*,*d*). For the black passing trajectory in figure 1 we note that the orbit-averaged value $\langle\partial B/\partial t\rangle_{\rm orbit}$ is negligible because this trajectory evenly observes positive and negative values of $\partial B/\partial t$, yielding negligible energy changes during the pump perturbations. Meanwhile, the green orbit is deeply trapped and as the perturbation grows this orbit will observe a negative value of $\langle\partial B/\partial t\rangle_{\rm orbit}$, resulting in a net cooling of deeply trapped electrons. The limiting case between trapped and passing electrons (not shown) is also interesting. Such marginally trapped electrons will with relatively low values of $v_\parallel/v$ reach the location where B is the strongest and $\partial B/\partial t$ is positive. As a result, the marginally trapped electrons spend a relatively long time in these regions resulting in positive values of $\langle\partial B/\partial t\rangle_{\rm orbit}$ and are therefore subject to energization as the standing-wave perturbation grows.

The distributions of the type predicted by (2.5) and displayed in figure 2(*c*,*d*) are consistent with electron distributions observed by MMS during bow-shock crossings (Lichko & Egedal 2020). The described energization of the marginally trapped electrons results in enhanced values of their phase-space density, and this is consistent with the distribution in figure 2(*d*) computed for the magnetic geometry in (2.2) with $\tilde{B}_m = B_m/B_0 = 1.5$. For a position $B/B_0 = 1.25$ near the peak magnetic field, the particles with $v_\parallel/v \simeq 0$ just inside the trapped–passing boundary are all marginally trapped with enhanced values of f. In figure 2(*c*) the distribution is evaluated at the minimum in B and here the region of $v_\parallel/v \simeq 0$ corresponds to deeply trapped (cooled) electrons with reduced values of f. Still, in the vicinity of the inferred trapped–passing boundaries, the distributions at reduced B include the marginally trapped orbits which in each case account for the enhanced values of f observed at pitch angles near the trapped–passing boundaries.

3. Simple picture of magnetic pumping with trapped electrons

The description above for the evolution of f does not include any net energizations because f in (2.5) will simply return to its original form after a full fluctuation period is completed. Energization by pumping therefore requires a pitch angle mixing process that changes the magnetic moment of the electrons in time. Considering figure 2(*b*), for $\tilde{B}_m = 1.5$ an electron with $\Lambda \simeq 0.7$ will be energized to a level of $\mathcal{E} \simeq 1.1\mathcal{E}_0$ as the magnetic field increases. For the most efficient scenario, such an electron may then pitch-angle scatter to a value of $\Lambda \simeq \Lambda_m = 2$, and as the perturbation reverts back to the uniform configuration with $B = B_0$, this electron will acquire an additional boost to reach $\mathcal{E} \simeq (1/0.5) \times 1.1\mathcal{E}_0 = 2.2\mathcal{E}_0$. Meanwhile, another electron may initially start out with $\Lambda = \Lambda_m$, and then scatter to $\Lambda \simeq 0.7$ as the magnetic field decreases, thus ending up with a lower energy of $\mathcal{E} \simeq \mathcal{E}_0/2.2$. As is characteristic of a second-order Fermi process, an important observation is here that the energy gain/loss is proportional to the particle's initial energy and that the step size (up or down) in energy is random.

The described diffusion process is characterized by a diffusion coefficient $D = (\Delta v)^2/\tau$, where Δv is the characteristic diffusive step in particle speed, while τ is the characteristic time associated with this step. Given $\Delta v \propto v$, we then have $D = \omega v^2 \mathcal{G}$, where $\mathcal{G}(\tilde{B}_m, \nu/\omega)$ is a dimensionless function of the magnetic perturbation size and the scattering rate ν normalized by the magnetic pump angular frequency ω. With Fick's law, the diffusion will cause a flux of particles in velocity space given by $\Gamma_v = -D\nabla f(v)$. From particle conservation it then follows that $\partial f/\partial t + \nabla \cdot \Gamma_v = 0$, which in spherical velocity

https://doi.org/10.1017/S0022377821001173 Published online by Cambridge University Press

space becomes

$$\frac{\partial f}{\partial t} = \frac{1}{v^2}\frac{\partial}{\partial v} v^2 D \frac{\partial f}{\partial v} - \frac{1}{3n}\frac{\partial n}{\partial t} v \frac{\partial f}{\partial v}. \tag{3.1}$$

In addition to diffusion by pumping, we here also include the term proportional to $\partial n/\partial t$ corresponding to changes in f due to compression of the plasma, a well-known effect that is also present in the Parker equation (Parker 1965; Montag *et al.* 2017). In the following sections we use the drift-kinetic framework to rigorously derive (3.1) and obtain an analytical expression for the function $\mathcal{G}$ describing the efficiency of the Fermi process.

Physically, the energy for particle energization is provided by mechanical work on the flux tube as captured by the term $p_\perp \boldsymbol{\nabla}_\perp \cdot \boldsymbol{v}_\perp$ in the standard two-fluid energy equation. In particular, for the regions where the magnetic field is decreasing the flux tube is expanding and the mechanical work during this phase will take energy out of the electrons. Meanwhile, as the field is expanding distributions of the type in figure 2(*c*) will form locally with reduced values of $p_\perp$. Pitch angle diffusion will naturally cause some level of isotropization, leading to enhanced values of $p_\perp$. Therefore more mechanical work is required to recompress the flux tube. As a consequence, when averaged over a full cycle a positive amount of mechanical work is delivered from the fluctuation to the electrons.

Based on the physical reasoning that leads to (3.1) and the similarity to magnetic pumping in an infinite, uniform flux-tube geometry (Lichko *et al.* 2017), it is possible to obtain quick approximations for the function $\mathcal{G}$ characterizing the rate of speed diffusion. However, the aim of the present paper is to provide a mathematically rigorous derivation starting from the drift-kinetic evolution equation for f, and then arrive at an equation similar in form to (3.1). This derivation will then in separate papers be generalized and combined with related heating mechanisms (Egedal *et al.* 2021) to account for magnetic pumping in more general magnetic perturbations including compressional waves of multiple amplitudes and phases.

4. Kinetic equation including pitch angle mixing

Following the analysis in Montag *et al.* (2017) and supplemented with additional discussion in Appendix A, for the assumed periodic geometry the drift-kinetic equation can be written as

$$\frac{\mathrm{d}f}{\mathrm{d}t} = \left.\frac{\partial f}{\partial t}\right|_{\Lambda,\mathcal{E}} + \frac{\mathrm{d}\Lambda}{\mathrm{d}t}\frac{\partial f}{\partial \Lambda} + \frac{\mathrm{d}\mathcal{E}}{\mathrm{d}t}\frac{\partial f}{\partial \mathcal{E}} = \nu \langle \mathcal{L} \rangle_x f. \tag{4.1}$$

For $\nu = 0$, (4.1) provides a representation of the collisionless fast transit-time limit, whereas for finite scattering frequencies $\nu \neq 0$ pitch angle mixing is included through the orbit average operator:

$$\langle \mathcal{L} \rangle_x = \frac{1}{\tau_b} \oint \frac{\mathcal{L}}{v_\parallel} \mathrm{d}l. \tag{4.2}$$

Here the local scattering can be characterized by, for example, the standard Lorentz operator $\mathcal{L} = \partial/\partial\xi(1-\xi^2)\partial/\partial\xi$, with $\xi = v_\parallel/v$. Furthermore, we have also introduced the orbit bounce time

$$\tau_b = \oint \frac{\mathrm{d}l}{v_\parallel} = 4\int_0^{L_b} \frac{1}{v_\parallel}\mathrm{d}x', \tag{4.3}$$

which together with its normalized form,

$$\tilde{\tau}_b = \frac{v\tau_b}{2L} = \frac{2v}{L}\int_0^{L_b} \frac{1}{v_\parallel}\mathrm{d}x', \tag{4.4}$$

https://doi.org/10.1017/S0022377821001173 Published online by Cambridge University Press

will become important in the following calculations.

We now introduce the dimensionless drive function $g(\Lambda, t)$ through the definition

$$g \equiv \frac{1}{\Lambda}\frac{\mathrm{d}\Lambda}{\mathrm{d}t} = -\frac{1}{\mathcal{E}}\frac{\mathrm{d}\mathcal{E}}{\mathrm{d}t}. \tag{4.5}$$

Here the expression in terms of $\mathcal{E}$ follows from the form of Λ in (2.4*a*,*b*), and we may then write the kinetic equation in (4.1) in the form

$$\frac{\partial f}{\partial t} = g\,\mathcal{E}\frac{\partial f}{\partial \mathcal{E}} - g\Lambda\frac{\partial f}{\partial \Lambda} + \nu\langle\mathcal{L}\rangle_x f, \tag{4.6}$$

which is equivalent to

$$\frac{\partial f}{\partial t} = g\,\frac{v}{2}\frac{\partial f}{\partial v} - g\Lambda\frac{\partial f}{\partial \Lambda} + \nu\langle\mathcal{L}\rangle_x f. \tag{4.7}$$

In order for (4.7) to be useful we need to obtain an expression for g related to the time evolution of the magnetic perturbation. For this we explore that the ratio J^2/μ is a constant of motion which has the special property that it is independent of $\mathcal{E}$ (Egedal 2002), and using j in (2.6) it follows that $0 = \mathrm{d}/\mathrm{d}t(J^2/\mu) = \mathrm{d}/\mathrm{d}t(j^2 B_0/\Lambda)$, such that

$$\frac{2}{j}\frac{\mathrm{d}j}{\mathrm{d}t} - \frac{1}{\Lambda}\frac{\mathrm{d}\Lambda}{\mathrm{d}t} = 0. \tag{4.8}$$

To evaluate the total differential of j we further notice that $j = j(\Lambda, t)$, while $\Lambda = \Lambda(t)$ such that

$$\frac{\mathrm{d}j}{\mathrm{d}t} = \frac{\partial j}{\partial t} + \frac{\mathrm{d}\Lambda}{\mathrm{d}t}\frac{\partial j}{\partial \Lambda}. \tag{4.9}$$

Combining (4.8) and (4.9) we find

$$g(\Lambda, t) = \frac{1}{\Lambda}\frac{\mathrm{d}\Lambda}{\mathrm{d}t} = \frac{2\partial j/\partial t}{j - 2\Lambda\,\partial j/\partial \Lambda} = \frac{2}{\tilde{\tau}_b}\frac{\partial j}{\partial t}. \tag{4.10}$$

Here we used

$$\tilde{\tau}_b = j - 2\Lambda\frac{\partial j}{\partial \Lambda}, \tag{4.11}$$

which is readily shown using

$$\frac{\tau_b}{m} = \left.\frac{\partial J}{\partial \mathcal{E}}\right|_{\mu}, \qquad \left.\frac{\partial}{\partial \mathcal{E}}\right|_{\mu} = \left.\frac{\partial}{\partial \mathcal{E}}\right|_{\Lambda} + 2\Lambda\frac{\partial}{\partial \Lambda}. \tag{4.12a,b}$$

Based on the definitions of j and $\tilde{\tau}_b$ in (2.6) and (4.4), and with the drive term g given in (4.10), the right-hand side of (4.7) is now readily evaluated numerically for any prescribed perturbation of the magnetic field, $B(x, t)$.

5. Particle conservation and a Krook scattering model

In our model, no electrons are permitted to 'leak' out of the considered flux tube, and particle conservation becomes a concept important to the derivations of the present framework. Without loss of generality, we assume that the magnetic field lines lie in the (x, z) plane, conveniently characterized by the flux function Ψ. It then also follows that the flux tube has constant width Δy_0 in the y direction. The total number of particles N within

https://doi.org/10.1017/S0022377821001173 Published online by Cambridge University Press

our flux tube of length L must be conserved, and using results of Montag *et al.* (2017) it follows that

$$N = \int f \,\mathrm{d}^3v \,\mathrm{d}^3x = \frac{2\pi\Delta y_0}{m^2}\int \mathrm{d}\mathcal{E}\int \mathrm{d}\mu \int \mathrm{d}\Psi\, \tau_b f. \tag{5.1}$$

The width of the tube in the z direction varies as $1/B$, but for the point $x = L/4$ the magnetic field is constant in time $B = B_0$, and we have $\Delta\Psi = B_0\Delta z_0$, where Δz_0 is the width of the flux tube at this location (and also the width of the initially uniform configuration). Furthermore, because $\tilde{\tau}_b = v\tau_b/(2L)$ and $\mathrm{d}\mathcal{E}\,\mathrm{d}\mu = m^2v^3\,\mathrm{d}v\,\mathrm{d}\Lambda/B_0$ we get

$$N = 4\pi\Delta y_0\Delta z_0 L\int v^2\,\mathrm{d}v\int \mathrm{d}\Lambda\tilde{\tau}_b f. \tag{5.2}$$

Guided by (5.2) we introduce the averaging operator

$$\langle(\dots)\rangle_\Lambda = \int \mathrm{d}\Lambda\,\tilde{\tau}_b(\dots), \tag{5.3}$$

where the range of integration over the full domain of Λ changes in time, $0 \le \Lambda \le \Lambda_m$ with $\Lambda_m = 1/B_{\min}(t)$. We define

$$F(v) = \langle f\rangle_\Lambda, \tag{5.4}$$

such that

$$N = \Delta y_0\Delta z_0 L\int 4\pi F(v)v^2\,\mathrm{d}v. \tag{5.5}$$

From (5.5) it is clear that $F(v)v^2\,\mathrm{d}v$ is proportional to the number of particles of the entire flux tube within a differential velocity interval $\mathrm{d}v$. It also follows that the volume V of the flux tube is given by

$$V = \Delta y_0\Delta z_0 L\,\langle 1\rangle_\Lambda = \Delta y_0\Delta z_0 L\int \mathrm{d}\Lambda\,\tilde{\tau}_b, \tag{5.6}$$

and $\langle 1\rangle_\Lambda$ therefore represents the relative change of the volume during the evolution of the magnetic perturbation.

If we assume a static magnetic configuration while integrating (4.1) for a long time compared to $1/\nu$, any initial distribution $f(\mathcal{E}, \Lambda)$ will pitch-angle mix into a form $f_{\mathrm{mixed}}(\mathcal{E})$ independent of Λ. Particle conservation at each energy then requires that $\langle f(\mathcal{E}, \Lambda)\rangle_\Lambda = \langle f_{\mathrm{mixed}}(\mathcal{E})\rangle_\Lambda = f_{\mathrm{mixed}}(\mathcal{E})\,\langle 1\rangle_\Lambda$. This observation motivates the construction of a Krook scattering operator:

$$\mathcal{L}_K f = -C_K\left(f - \frac{\langle f\rangle_\Lambda}{\langle 1\rangle_\Lambda}\right), \tag{5.7}$$

which compared with the orbit-averaged Lorentz operator, $\langle\mathcal{L}\rangle_x$, is much better suited for analytical calculations. The factor C_K was introduced by Lichko & Egedal (2020) to calibrate $\mathcal{L}_K$ to have scattering efficiency similar to $\langle\mathcal{L}\rangle_x$, as a function of the velocity space scale length of the anisotropic features in $f(\mathcal{E}, \Lambda)$. For example, for situations where the anisotropy of the local distribution is dominated by the $P_l(v_\parallel/v)$ Legendre polynomial of order l, the appropriate calibration factor becomes $C_K = l(l+1)$.

https://doi.org/10.1017/S0022377821001173 Published online by Cambridge University Press

6. Kinetic model of magnetic pumping

In the present section we derive an evolution equation for a slowly evolving background distribution energized by the pumping process. Consistent with the Krook operator in (5.7) the isotropic part of the distribution is given by

$$f_0 = \frac{\langle f \rangle_\Lambda}{\langle 1 \rangle_\Lambda} = \frac{1}{\langle 1 \rangle_\Lambda} F(v). \tag{6.1}$$

During each pump cycle the volume of the flux tube may change as characterized by $\langle 1 \rangle_\Lambda$, and f_0 therefore does not necessarily represent a slowly evolving distribution. For this reason it turns out that the pumping process is better characterized in terms of the Λ-averaged distribution, $F(v) = \langle f \rangle_\Lambda = f_0 \langle 1 \rangle_\Lambda$, introduced above in (5.4).

6.1. *Limit of strong scattering, $\nu \gg \omega$*

Our aim is first to derive an equation for $\partial F/\partial t$, which describes the evolution of $F(v, t)$ due to magnetic pumping in the limit of strong scattering, $\nu \gg \omega$, and small magnetic perturbation amplitudes. By direct differentiation of (5.4) we obtain

$$\frac{\partial F}{\partial t} = \left\langle \frac{\partial f}{\partial t} \right\rangle_\Lambda + \int \mathrm{d}\Lambda \, \frac{\partial \tilde{\tau}_b}{\partial t} f + \tilde{\tau}_b f|_{\Lambda_m} \dot{\Lambda}_m, \tag{6.2}$$

where $\dot{\Lambda}_m = \partial \Lambda_m / \partial t$. To evaluate the various terms in (6.2) we introduce an expansion for f for which the first term is the isotropic component:

$$f = f_0(t, v) + f_1(t, v, \Lambda) + \cdots . \tag{6.3}$$

We here assume a small-amplitude ordering $\Delta B/B \ll 1$, such that $|g| \simeq |f_1| \ll |f_0|$, and the kinetic equation in (4.7) with the Krook approximation in (5.7) then yields an approximate equation for f_1:

$$\frac{\partial f_1}{\partial t} = h \frac{v}{2} \frac{\partial f_0}{\partial v} + \nu \mathcal{L}_K f_1, \tag{6.4}$$

where

$$h \equiv g - (\langle g \rangle_\Lambda / \langle 1 \rangle_\Lambda). \tag{6.5}$$

Furthermore, by introducing the ordering $\nu/\omega \gg 1$, we can ignore $\partial f_1/\partial t$ on the left-hand side of (6.4), such that

$$f_1 = \frac{h}{\nu C_K} \frac{v}{2} \frac{\partial f_0}{\partial v}. \tag{6.6}$$

Considering again (6.2) we may now evaluate the two last terms on the right-hand side. First we observe that

$$\int \mathrm{d}\Lambda f \frac{\partial \tilde{\tau}_b}{\partial t} = f_0 \int \mathrm{d}\Lambda \frac{\partial \tilde{\tau}_b}{\partial t} + \frac{1}{\nu C_K} \int h \frac{\partial \tilde{\tau}_b}{\partial t} \mathrm{d}\Lambda \, \frac{v}{2} \frac{\partial}{\partial v} f_0, \tag{6.7}$$

while

$$\tilde{\tau}_b f|_{\Lambda_m} \dot{\Lambda}_m = \tilde{\tau}_b \dot{\Lambda}_m \big|_{\Lambda_m} f_0 + \tilde{\tau}_b h \dot{\Lambda}_m \big|_{\Lambda_m} \frac{1}{\nu C_K} \frac{v}{2} \frac{\partial f_0}{\partial v}, \tag{6.8}$$

https://doi.org/10.1017/S0022377821001173 Published online by Cambridge University Press

such that (6.2) becomes

$$\frac{\partial F}{\partial t} = \left\langle \frac{\partial f}{\partial t} \right\rangle_\Lambda + f_0 \int \mathrm{d}\Lambda \frac{\partial \tilde{\tau}_b}{\partial t} + T \frac{1}{\nu C_K} \frac{v}{2} \frac{\partial f_0}{\partial v}, \tag{6.9}$$

where

$$T = \int h \frac{\partial \tilde{\tau}_b}{\partial t} \mathrm{d}\Lambda + \tilde{\tau}_b h|_{\Lambda_m} \dot{\Lambda}_m. \tag{6.10}$$

To evaluate $\langle \partial f/\partial t \rangle_\Lambda$ we insert $f = f_0 + f_1$ back into (4.7):

$$\frac{\partial f}{\partial t} = g \frac{v}{2} \frac{\partial f_0 + f_1}{\partial v} - g\Lambda \frac{\partial f_1}{\partial \Lambda} - \nu C_K f_1. \tag{6.11}$$

Then, using $\langle f_1 \rangle_\Lambda = 0$ and $\langle k f_0 \rangle_\Lambda = f_0 \langle k \rangle_\Lambda$ we find

$$\begin{aligned} \left\langle \frac{\partial f}{\partial t} \right\rangle_\Lambda &= \langle g \rangle_\Lambda \frac{v}{2} \frac{\partial}{\partial v} f_0 + \frac{1}{\nu C_K} \langle gh \rangle_\Lambda \frac{v}{2} \frac{\partial}{\partial v} \frac{v}{2} \frac{\partial}{\partial v} f_0 - \frac{1}{\nu C_K} \left\langle g\Lambda \frac{\partial h}{\partial \Lambda} \right\rangle_\Lambda \frac{v}{2} \frac{\partial}{\partial v} f_0 \\ &= \langle g \rangle_\Lambda \frac{v}{2} \frac{\partial}{\partial v} f_0 + \frac{1}{\nu C_K} \langle gh \rangle_\Lambda \frac{1}{4v^2} \frac{\partial}{\partial v} v^4 \frac{\partial}{\partial v} f_0 - \frac{1}{\nu C_K} T \frac{v}{2} \frac{\partial}{\partial v} f_0. \end{aligned} \tag{6.12}$$

Here the last form of (6.12) assumes that

$$\frac{3}{2} \langle gh \rangle_\Lambda = -\left\langle g\Lambda \frac{\partial h}{\partial \Lambda} \right\rangle_\Lambda + T, \tag{6.13}$$

which is proved below. In addition we also verify a similar expression needed in the next few steps:

$$\frac{3}{2} \langle g \rangle_\Lambda = \int \mathrm{d}\Lambda \frac{\partial \tilde{\tau}_b}{\partial t} + \tilde{\tau}_b|_{\Lambda_m} \dot{\Lambda}_m = \frac{\partial}{\partial t} \langle 1 \rangle_\Lambda . \tag{6.14}$$

To prove (6.13) and (6.14) we recall that $\tilde{\tau}_b g = 2\partial j/\partial t$, $j = \tilde{\tau}_b + 2\Lambda \partial j/\partial \Lambda$ and $j|_{\Lambda_m} = 0$. As an intermediate result, for any $G = G(t, \Lambda)$ it then follows that

$$\begin{aligned} \int \mathrm{d}\Lambda \frac{\partial}{\partial \Lambda} G\Lambda \frac{\partial j}{\partial t} &= \frac{\partial}{\partial t} \cancelto{0}{\int \mathrm{d}\Lambda \frac{\partial}{\partial \Lambda} G\Lambda j} - \cancelto{0}{\int \mathrm{d}\Lambda \frac{\partial}{\partial \Lambda} \Lambda j \frac{\partial G}{\partial t}} - \dot{\Lambda}_m \frac{\partial}{\partial \Lambda} G\Lambda j \Big|_{\Lambda_m} \\ &= -\dot{\Lambda}_m \left[\cancelto{0}{\left(\frac{\partial}{\partial \Lambda} G\Lambda \right) j \Big|_{\Lambda_m}} + G\Lambda \frac{\partial}{\partial \Lambda} j \Big|_{\Lambda_m} \right] \\ &= -\dot{\Lambda}_m G \frac{j - \tilde{\tau}_b}{2} \Big|_{\Lambda_m} = \frac{1}{2} G \dot{\Lambda}_m \tilde{\tau}_b|_{\Lambda_m} . \end{aligned} \tag{6.15}$$

We now consider $\langle gh \rangle_\Lambda = 2 \int \mathrm{d}\Lambda h \partial j/\partial t$, and use (6.15) with $G = h$ to simplify the expressions:

$$\begin{aligned} \langle gh \rangle_\Lambda &= 2 \int \mathrm{d}\Lambda h \frac{\partial \tilde{\tau}_b}{\partial t} + 4 \int d\Lambda \, \Lambda h \frac{\partial}{\partial \Lambda} \frac{\partial j}{\partial t} \\ &= 2 \int \mathrm{d}\Lambda h \frac{\partial \tilde{\tau}_b}{\partial t} + 4 \int \mathrm{d}\Lambda \frac{\partial}{\partial \Lambda} h\Lambda \frac{\partial j}{\partial t} - 4 \int \mathrm{d}\Lambda h \frac{\partial j}{\partial t} - 4 \int \mathrm{d}\Lambda \frac{\partial j}{\partial t} \Lambda \frac{\partial}{\partial \Lambda} h \\ &= 2 \int \mathrm{d}\Lambda h \frac{\partial \tilde{\tau}_b}{\partial t} + 2h\dot{\Lambda}_m \tilde{\tau}_b|_{\Lambda_m} - 2 \langle gh \rangle_\Lambda - 2 \left\langle g\Lambda \frac{\partial h}{\partial \Lambda} \right\rangle_\Lambda . \end{aligned} \tag{6.16}$$

https://doi.org/10.1017/S0022377821001173 Published online by Cambridge University Press

From here (6.13) is readily obtained.

Similarly, this time with $G = 1$ in (6.15), we get

$$\begin{aligned}\langle g\rangle_\Lambda &= 2\int \mathrm{d}\Lambda \frac{\partial \tilde{\tau}_b}{\partial t} + 4\int \mathrm{d}\Lambda\, \Lambda \frac{\partial}{\partial \Lambda}\frac{\partial j}{\partial t}\\ &= 2\int \mathrm{d}\Lambda \frac{\partial \tilde{\tau}_b}{\partial t} + 4\int \mathrm{d}\Lambda \frac{\partial}{\partial \Lambda}\Lambda\frac{\partial j}{\partial t} - 4\int \mathrm{d}\Lambda \frac{\partial j}{\partial t}\\ &= 2\int \mathrm{d}\Lambda \frac{\partial \tilde{\tau}_b}{\partial t} + 2\dot{\Lambda}_m\, \tilde{\tau}_b|_{\Lambda_m} - 2\langle g\rangle_\Lambda\,, \end{aligned} \tag{6.17}$$

and from here (6.14) follows directly.

Inserting (6.12) into (6.9) and using (6.14) together with $f_0 = F/\langle 1\rangle_\Lambda$ yields the desired evolution equation for $F(v,t)$:

$$\frac{\partial F}{\partial t} = \frac{1}{\nu C_K}\frac{\langle gh\rangle_\Lambda}{\langle 1\rangle_\Lambda}\frac{1}{4v^2}\frac{\partial}{\partial v}v^4\frac{\partial}{\partial v}F + \frac{\langle g\rangle_\Lambda}{2\langle 1\rangle_\Lambda}\frac{1}{v^2}\frac{\partial}{\partial v}v^3 F. \tag{6.18}$$

Again, the result in (6.18) is obtained in the limit $\nu \gg \omega$ and describes the evolution of a near-isotropic electron plasma. Because $F|_{v=\infty} = 0$, through integration by parts it is readily seen that $\int \partial F/\partial t\, v^2\, \mathrm{d}v = 0$ and (6.18) is therefore consistent with particle conservation. The anisotropic features in f are given by f_1 proportional to $h/(\nu C_k)$ with h given in (6.5). The term proportional to $\langle gh\rangle_\Lambda/(\nu C_k)$ then accounts for the bi-linear interaction between $h/(\nu C_k)$ and the drive g, yielding velocity diffusion akin to Fermi acceleration.

To understand the term in (6.18) proportional to $\langle g\rangle_\Lambda/(2\langle 1\rangle_\Lambda)$ we recall (6.14), and note again that $\langle 1\rangle_\Lambda$ is proportional to the volume of the flux tube, such that $3/2\,\langle g\rangle_\Lambda/\langle 1\rangle_\Lambda = \partial \log\langle 1\rangle_\Lambda/\partial t$ is the rate of relative compression of the flux tube. In terms of the average plasma density $n \equiv N/(\Delta y_0 \Delta z_0 L\langle 1\rangle_\Lambda)$, it follows that $\langle g\rangle_\Lambda/(2\langle 1\rangle_\Lambda) = -(1/3)\partial\log(n)/\partial t$, and it is then clear that this last term of (6.18) accounts for compressional heating of an isotropic plasma, as is familiar from the similar term in the Parker equation (Parker 1965) and also included in (3.1) above.

6.2. *General case, including arbitrary scattering levels*

Above, we solved (6.4) in the limit $\nu/\omega \gg 1$ to get an approximate solution for f_1. Still for $\Delta B/B_0 \ll 1$, to address the more general case with no restrictions on ν/ω, we apply Fourier expansions of g, h and f_1:

$$\begin{aligned} g(\eta,t) &= g^1(\eta)\mathrm{e}^{\mathrm{i}\omega t} + g^2(\eta)\mathrm{e}^{2\mathrm{i}\omega t} + \cdots,\\ h(\eta,t) &= h^1(\eta)\mathrm{e}^{\mathrm{i}\omega t} + h^2(\eta)\mathrm{e}^{2\mathrm{i}\omega t} + \cdots,\\ f_1(\eta,t) &= f_1^1(\eta)\mathrm{e}^{\mathrm{i}\omega t} + f_1^2(\eta)\mathrm{e}^{2\mathrm{i}\omega t} + \cdots. \end{aligned} \tag{6.19}$$

For this to be meaningful we have introduced the new variable η, for which the range is constant in time $0 \le \eta \le 1$. Furthermore, because

$$\int h\tilde{\tau}_b\, \mathrm{d}\Lambda = 0, \tag{6.20}$$

this constraint must be fulfilled by each of the terms in the sum

$$\int h^n \tilde{\tau}_b \frac{\partial \Lambda}{\partial \eta}\mathrm{d}\eta = 0. \tag{6.21}$$

https://doi.org/10.1017/S0022377821001173 Published online by Cambridge University Press

For the general case where $\tilde{\tau}_b$ depends on (Λ, t), the constraint implies that $\tilde{\tau}_b \partial\Lambda/\partial\eta = K(t)$, where $K(t)$ is an arbitrary function independent of Λ. Imposing further that $0 \leq \eta \leq 1$ and $\eta = 1$ for $\Lambda = 0$, there is then only one definition of η available:

$$\frac{\partial\eta}{\partial\Lambda} = -\frac{\tilde{\tau}_b}{\langle 1\rangle_\Lambda}, \quad \eta = 1 - \frac{1}{\langle 1\rangle_\Lambda}\int_0^\Lambda \tilde{\tau}_b \,\mathrm{d}\Lambda'. \tag{6.22a,b}$$

To emphasize some properties of η, the averaging operator in (5.3) may be expressed as $\langle(\dots)\rangle_\Lambda = \langle 1\rangle_\Lambda \int(\dots)\,\mathrm{d}\eta$, and for the uniform flux tube we observe that $\eta = v_\parallel/v$.

Returning to (6.4) we recall that this equation for f_1 was derived with (v, Λ) as the independent velocity space variables. In principle, with $f_1 = f_1(v, \eta, t)$ a new term will then occur as we note that

$$\left.\frac{\partial f_1}{\partial t}\right|_{\Lambda,\mathcal{E}} = \left.\frac{\partial f_1}{\partial t}\right|_{\eta,\mathcal{E}} + \left.\frac{\partial\eta}{\partial t}\right|_\Lambda \frac{\partial f_1}{\partial\eta}. \tag{6.23}$$

However, because $\partial\eta/\partial t|_\Lambda = 0$ for $\Delta B = 0$, the term $\partial\eta/\partial t|_\Lambda\, \partial f_1/\partial\eta$ is of second order in $\Delta B/B_0$ and can be ignored. This permits us to write $\partial f_1/\partial t = \mathrm{i}\omega f_1$, and similar to (6.4) for the separate frequencies the equation for f_1^n then reads

$$\mathrm{i}n\omega f_1^n = h^n \frac{v}{2}\frac{\partial f_0}{\partial v} - C_K \nu f_1^n, \tag{6.24}$$

such that $f_1 = \sum_n f_1^n$, with

$$f_1^n = K_n \frac{v}{2}\frac{\partial f_0}{\partial v}, \quad K_n = \frac{h^n(-\mathrm{i}n\omega + C_K\nu)}{n^2\omega^2 + C_K^2\nu^2}. \tag{6.25a,b}$$

Using (6.25*a*,*b*) in place of (6.6), we may now follow the same steps that led from (6.6) to (6.18). Analogous to before when pumping was driven by $\langle\langle g f_1\rangle_\Lambda\rangle_t$, we find that parts of f_1^n are in phase with g^n causing the time average $\langle\langle g^n f_1^n\rangle_\Lambda\rangle_t$ to become finite. An equation for the slowly varying $F(v, t)$ is then obtained as

$$\left.\begin{aligned} \frac{\partial F}{\partial t} &= \frac{1}{v^2}\frac{\partial}{\partial v}\left(v^2 D\frac{\partial}{\partial v}F\right), \quad D = \omega v^2 \mathcal{G}, \\ \mathcal{G}\left(\frac{\nu C_K}{\omega}\right) &\equiv \frac{1}{4}\sum_n \frac{\nu C_K/\omega}{n^2 + (\nu C_k/\omega)^2}\langle\langle g^n h^n\rangle_\Lambda\rangle_t, \\ \langle\langle g^n h^n\rangle_\Lambda\rangle_t &\equiv \left\langle \frac{\langle \mathrm{Re}(g^n \mathrm{e}^{\mathrm{i}n\omega t})\mathrm{Re}(h^n \mathrm{e}^{\mathrm{i}n\omega t})\rangle_\Lambda}{\omega^2\langle 1\rangle_\Lambda}\right\rangle_t. \end{aligned}\right\} \tag{6.26}$$

The efficiency of magnetic pumping with trapped electrons is characterized by (6.26) and is now readily evaluated numerically for any periodic magnetic perturbation, oscillating as a standing wave as a function of time. We may also generalize (6.26) to account for slow flux-tube compression simply by including the term proportional to $\langle g\rangle_\Lambda$ in (6.18).

6.3. *Evaluation of the pumping efficiency*

The model in (6.26) is verified by evaluating its predictions as a function of $\nu C_K/\omega$ for a number of discrete perturbation magnitudes, parameterized by $\Delta B/B_0$ in (2.1). These predictions are then compared with results obtained by numerically integrating

https://doi.org/10.1017/S0022377821001173 Published online by Cambridge University Press

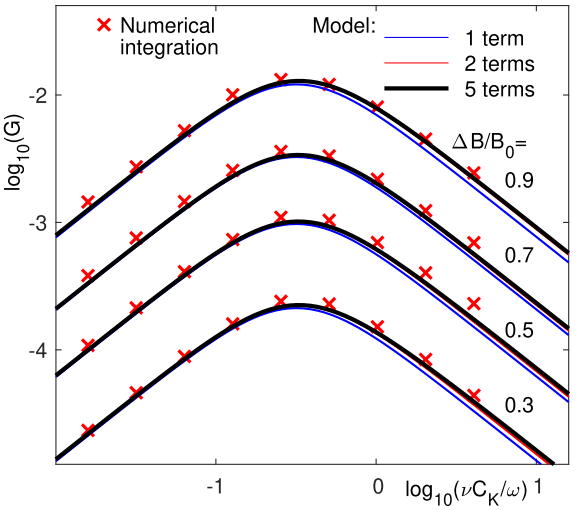

FIGURE 3. Solid lines show predictions for $\mathcal{G}$ calculated with $\Delta B/B_0 \in \{0.3, 0.5, 0.7, 0.9\}$, and including the first one, two and five finite terms of the sum in (6.26). For comparison, the red crosses are obtained by numerical integration of (4.7), using equation (7) of Lichko & Egedal (2020) to estimate $\mathcal{G}$.

(4.7) directly, and using equation (7) of Lichko & Egedal (2020) to estimate $\mathcal{G}$ from the numerical evolution of $f(v, t)$. This integration can be carried out with $\langle \mathcal{L} \rangle_x$ based on the Lorentz form or the Krook form in (5.7), but for direct comparison with the model in (6.26) we here only consider results obtained using the Krook representation.

The results of the numerical integration of (4.7) are represented by the red crosses in figure 3. In comparison, the lines are obtained from (6.26) based on the following steps. For a given value of $\Delta B/B_0$ the spatial and temporal variation of B is given through (2.1) and (2.2). This then permits direct evaluation of j and $\tilde{B}$ as a function of (Λ, t) using (2.6) and (4.4). Evaluation of g and h in (4.10) and (6.5) then follows, from which their Fourier expansions in (6.19) are determined. All quantities needed for evaluating the required Λ and t averages of (6.26) thereby become available. Given that the time dependency of the configuration is set through the $|\sin(\omega t)|$ term in (2.1), only even terms of n contribute in (6.26). The lines in figure 3 represent the result of the first one, two and five finite terms in the expansion of frequencies. The red lines obtained with $n \in \{2, 4\}$ are mostly hidden behind the black lines obtained with $n \in \{2, 4, 6, 8, 10\}$ demonstrating the rapid conversion of the expansion.

For all values of $\Delta B/B_0$ and $\nu C_K/\omega$ the predictions of (6.26) are observed to be in good agreement with the numerical integration results. Lichko & Egedal (2020) further shows that the model based on the Krook scattering operator also is in agreement with numerical results obtained with the Lorentz form of $\langle \mathcal{L} \rangle_x$ (defined as the orbit average of the local $\mathcal{L} = \partial/\partial\xi(1-\xi^2)\partial/\partial\xi$). This agreement, however, requires that the value of C_K be adjusted to become large at small values of $\Delta B/B_0$, where the pitch angle scale size of the features in f_1 are the smallest and most efficiently scattered by $\langle \mathcal{L} \rangle_x$. Curve fitting yields the following easy-to-evaluate form accurate for the range of $0 \le \Delta B/B \lesssim 0.9$:

$$\mathcal{G}\left(\frac{\nu C_K}{\omega}\right) \simeq \frac{0.02\,\nu C_K/\omega}{4 + (\nu C_k/\omega)^2}\left[\left(\frac{\Delta B}{B}\right)^{2.6} + 3\left(\frac{\Delta B}{B}\right)^{5.6}\right]. \tag{6.27}$$

https://doi.org/10.1017/S0022377821001173 Published online by Cambridge University Press

This form based on numerical results with the Krook scattering operator is somewhat different from the similar expression in Lichko & Egedal (2020) for results based on the Lorentz form of the scattering operator. These differences are mainly due to a normalization mistake, as the expression and curves in Lichko & Egedal (2020) were multiplied up by an erroneous factor of π (still, the model was correctly applied in the analysis of the MMS observations).

Given the model was derived through an expansion $f = f_0 + f_1 + \cdots$ with $f_1 \ll f_0$, the good agreement between the numerical integration results and those of (6.26) is perhaps surprising. Strictly, agreement should only be expected for $\nu C_K/\omega \gg 1$ and/or $\Delta B/B_0 \ll 1$, which ensures that $f_1 \ll f_0$. For example, for $\nu C_K/\omega \ll 1$ and $\Delta B/B_0 = 0.5$ distributions similar to those in figure 2 will occur where the anisotropic part described by f_1 is comparable in magnitude to f_0. For this limit where $\nu C_K/\omega \lesssim 1$ a model can likely be obtained where again $f = f_0 + f_1 + \cdots$, but with $f_0 = f_0(J, \mu)$ similar to (2.5). We expect that such a framework will provide results similar to (6.26), but the analysis is beyond the scope of the present paper.

7. Summary and conclusions

Lichko & Egedal (2020) developed a new magnetic pumping model which successfully accounts for detailed *in situ* MMS observations of electron energization at the Earth's bow shock. In the present paper we provide a detailed mathematical derivation of the model obtained by exploring the fast transit-time limit of a drift-kinetic plasma description, including the effects of electrons becoming trapped in the magnetic perturbations. While the model is derived with an assumption of small magnetic perturbations, it also accurately accounts for the heating rates at large magnetic perturbation amplitudes. This is evident with a comparison of the result of the model with those obtained by direct numerical integration of the drift-kinetic equation. Despite the highly idealized form of the magnetic geometry considered, the model provides an accurate description of the anisotropic form and energization of electron distributions observed at the Earth's bow shock. The mathematical framework may also serve as a starting point for additional studies, generalizing the model to more complicated and realistic scenarios where the magnetic perturbations are comprised of multiple waves with variable amplitudes and propagation directions.

We emphasize the role of magnetic trapping for magnetic pumping to become effective for superthermal electrons. Without trapping the rapid thermal streaming of electrons along magnetic field lines renders pumping ineffective for electron energization. Meanwhile, even small-amplitude magnetic perturbations can trap a significant fraction of the electrons, and given that the magnetic mirror force is proportional to $\mathcal{E}_\perp$, this trapping applies to all energies for which the electrons are magnetized. Particularly important for space and astrophysical applications, the present model represents a second-order Fermi process consistent with the generation of electron distributions with energetic power-law tails.

Acknowledgements

Editor William Dorland thanks the referees for their advice in evaluating this article.

Funding

This work was supported in part by NASA HERMES DRIVE Science Center grant no. 80NSSC20K0604. Contributions from E.L. were also supported by the Department of Defense (DoD) through the National Defense Science & Engineering Graduate Fellowship (NDSEG) Program and the NASA Earth and Space Science Fellowship.

Declaration of interests

The authors report no conflict of interest.

Appendix A

The form of the kinetic equation applied in our analysis as well as Jean's theorem (Jeans 1915) can be recovered using the multiple-time-scale perturbation analysis method introduced by Davidson (1972), which, by way of examples, also is applied by Cordey (1976) and Kolesnichenko *et al.* (1995). For the present problem, the fundamental assumption is that the frequency of the bounce motion of the electrons far exceeds the collision frequency, as well as the frequency for variations in the magnetic field. We define the small expansion parameter, ϵ_p, as the ratio of these two quantities, $\epsilon_p = \tau_b/\tau_*$, where τ_b is the characteristic time of particle motion in the magnetic field, or the bounce time, and τ_* is the characteristic time for particle collisions. For the kinetic equation

$$\frac{\mathrm{d}f}{\mathrm{d}t} = C(f) \equiv \frac{G}{\tau_*} \tag{A1}$$

we introduce independent time variables of the form

$$\tau^{(0)} = t/\tau_b, \quad \tau^{(n)} = (\epsilon_p)^n \tau^{(0)}, \quad \text{where } n = 1, 2, \ldots \tag{A2}$$

The time derivative then takes the form

$$\frac{\mathrm{d}}{\mathrm{d}t} = \frac{1}{\tau_b}\frac{\mathrm{d}}{\mathrm{d}\tau^{(0)}} + \frac{\epsilon_p}{\tau_b}\frac{\mathrm{d}}{\mathrm{d}\tau^{(1)}} + \cdots \tag{A3}$$

and the distribution function is expanded in terms of the new independent variables:

$$f = f_0(\tau^{(0)}, \tau^{(1)}, \ldots) + \epsilon_p f_1(\tau^{(0)}, \tau^{(1)}, \ldots) + \cdots . \tag{A4}$$

With these expansions, to the lowest order in ϵ_p we obtain the equation

$$\frac{\mathrm{d}f_0}{\mathrm{d}\tau^{(0)}} = 0. \tag{A5}$$

This equation can be solved by integrating along its characteristics, which are the equations for the particle orbits. The characteristics are given by $x = x(\alpha_1, \alpha_2, \ldots, \alpha_N, t)$, where $\alpha_1, \alpha_2, \ldots, \alpha_N$ are the integrals of motion. Consistent with Jean's theorem, the solution then becomes

$$f_0 = g(\alpha_1, \alpha_2, \ldots, \alpha_6), \tag{A6}$$

where g is an arbitrary function.

To the next order in ϵ_p, we have the equation

$$\frac{\mathrm{d}f_1}{\mathrm{d}\tau^{(0)}} = -\frac{\mathrm{d}f_0}{\mathrm{d}\tau^{(1)}} + G. \tag{A7}$$

To avoid time secularities, i.e. unphysical solutions to the kinetic equation, we have the solvability condition

$$\int_0^{\tau_b} \left(\frac{\mathrm{d}f_0}{\mathrm{d}\tau^{(1)}} - G \right) \mathrm{d}\tau^{(0)} = 0. \tag{A8}$$

https://doi.org/10.1017/S0022377821001173 Published online by Cambridge University Press

This equation can be expressed as

$$\frac{\partial f_0}{\partial t} = \frac{1}{\tau_*}\int_0^{\tau_b} G\frac{\mathrm{d}t}{\tau_b}. \tag{A9}$$

Equation (A9) is the analogue of the orbit average of the scattering operator in (4.1). We notice that (4.1) has additional terms on the left-hand side of the equation. This is due to the fact that while $\mathcal{E}$ and Λ are constants of motion during a single orbit transit, they are not over the time scale of the pumping cycle. Meanwhile, because $\partial/\partial t|_{\mu,J} = \partial/\partial t|_{\Lambda,\mathcal{E}} + \mathrm{d}\Lambda/\mathrm{d}t\,\partial/\partial\Lambda + \mathrm{d}\mathcal{E}/\mathrm{d}t\,\partial/\partial\mathcal{E}$, recasting (4.1) with μ and $J = \oint v_\parallel\,\mathrm{d}l$ as the principal variables reproduces (A9) exactly.

REFERENCES

ALFVEN, H. 1950 On the solar origin of cosmic radiation. 2. *Phys. Rev*. **77** (3), 375–379.

BARNES, A. 1966 Collisionless damping of hydromagnetic waves. *Phys. Fluids* **9** (8), 1483.

BERGER, J. M. 1958 Heating of a confined plasma by oscillating electromagnetic fields. *Phys. Fluids* **1**, 301–307.

CORDEY, J. G. 1976 Effects of particle trapping on the slowing-down of fast ions in a toroidal plasma. *Nucl. Fusion* **16** (3), 499–507.

DAVIDSON, R. C. 1972 *Methods in Nonlinear Plasma Theory*. Academic.

EGEDAL, J. 2002 A drift kinetic approach to stationary collisionless magnetic reconnection in an open CUSP plasma. *Phys. Plasmas* **9** (4), 1095–1103.

EGEDAL, J., MONKHORST, H., LICHKO, E. & MONTAG, P. 2018 Theory of ion dynamics and heating by magnetic pumping in FRC plasma. *Phys. Plasmas* **25** (7), 072510.

EGEDAL, J., SCHROEDER, J. & LICHKO, E. 2021 Parallel velocity mixing yielding enhanced electron heating during magnetic pumping. *J. Plasma Phys*. **87** (2), 905870116.

JEANS, J. H. 1915 On the theory of star-streaming and the structure of the universe. *Mon. Not. R. Astron. Soc* **76** (1), 70–84.

KOLESNICHENKO, Y. I., LISAK, M., LUTSENKO, V. V. & WISING, F. 1995 Space and velocity distributions of fast ions in magnetically confined plasmas. *Plasma Phys. Control. Fusion* **37** (1), 363–386.

LICHKO, E. & EGEDAL, J. 2020 Magnetic pumping model for energizing superthermal particles applied to observations of the Earth's bow shock. *Nat. Commun*. **11** (1), 2942.

LICHKO, E., EGEDAL, J., DAUGHTON, W. & KASPER, J. 2017 Magnetic pumping as a source of particle heating and power-law distributions in the solar wind. *Astrophys. J. Lett*. **850** (2), L17.

MONTAG, P., EGEDAL, J., LICHKO, E. & WETHERTON, B. 2017 Impact of compressibility and a guide field on fermi acceleration during magnetic island coalescence. *Phys. Plasmas* **24** (1), 062906.

PARKER, E. N. 1965 Passage of energetic charged particles through interplanetary space. *Planet. Space Sci*. **13** (1), 9–49.

SCHLUTER, A. 1957 Der gyro-relaxations-effekt. *Z. Naturforsch*. **12** (10), 822–825.

STIX, T. H. 1992 *Waves in Plasmas*. Springer.

https://doi.org/10.1017/S0022377821001173 Published online by Cambridge University Press